

# Frequency-aware Event Cloud Network

Hongwei Ren<sup>1\*</sup>, Fei Ma<sup>2\*</sup>, Xiaopeng Lin<sup>1</sup>, Yuetong Fang<sup>1</sup>, Hongxiang Huang<sup>1</sup>, Yulong Huang<sup>1</sup>, Yue Zhou<sup>1</sup>, Haotian Fu<sup>1</sup>, Ziyi Yang<sup>1</sup>, Fei Richard Yu<sup>3,4</sup>, Bojun Cheng<sup>1†</sup>

## Abstract

Event cameras are biologically inspired sensors that emit events asynchronously with remarkable temporal resolution, garnering significant attention from both industry and academia. Mainstream methods favor frame and voxel representations, which reach a satisfactory performance while introducing time-consuming transformation, bulky models, and sacrificing fine-grained temporal information. Alternatively, Point Cloud representation demonstrates promise in addressing the mentioned weaknesses, but it ignores the polarity information, and its models have limited proficiency in abstracting long-term events' features. In this paper, we propose a frequency-aware network named FECNet that leverages Event Cloud representations. FECNet fully utilizes 2S-1T-1P Event Cloud by innovating the event-based Group and Sampling module. To accommodate the long sequence events from Event Cloud, FECNet embraces feature extraction in the frequency domain via the Fourier transform. This approach substantially extinguishes the explosion of Multiply Accumulate Operations (MACs) while effectively abstracting spatial-temporal features. We conducted extensive experiments on event-based object classification, action recognition, and human pose estimation tasks, and the results substantiate the effectiveness and efficiency of FECNet. Our code is available at <https://github.com/rhwxmx/FECNet>

## 1. Introduction

Event cameras represent a revolutionary advancement in the field of computer vision [16, 24]. Unlike traditional frame-based cameras that capture images at fixed intervals, event cameras operate asynchronously, detecting local changes in illumination that exceed a predetermined threshold and generating events independently at the pixel level [37]. This fundamental difference allows them to achieve exceptional performance characterized by high dynamic range, low la-

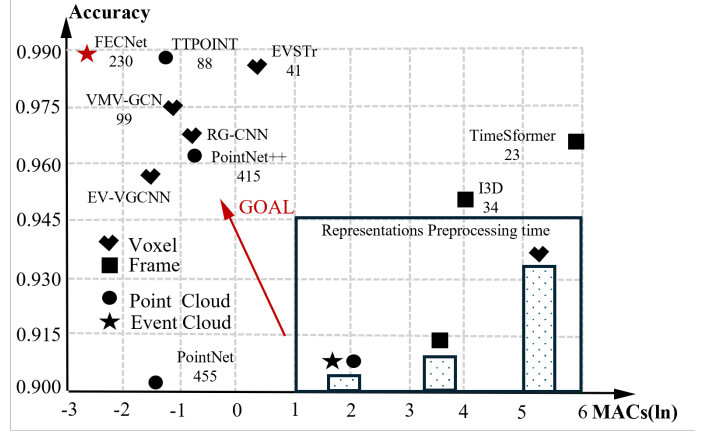


Figure 1. Gain of FECNet on DVS128 Gesture. The horizontal axis represents the MACs after taking  $\ln$ , the vertical axis represents accuracy, the different shapes denote representations, and the number beside the shape is throughput (FPS).

teness, and low power consumption [34]. Consequently, event cameras demonstrate superior effectiveness in capturing high-speed motion and rapid scene dynamics, generating outputs in microsecond resolution, which far surpasses the frame rate of conventional cameras [12]. These attributes make it particularly significant for robotics, security, and autonomous driving applications [30].

The raw events generated by event cameras are represented by four dimension coordinates, which comprise the spatial coordinate  $(x, y)$ , timestamps  $t$ , and polarity  $p$  of each event occurrence [48]. Due to the boom in deep learning algorithms in computer vision, most efforts in event-based vision primarily focus on converting raw events into frame-based or voxel-based representations, employing established backbones to accomplish various tasks, such as VGG [46], ResNet [19], and Transformer [15]. Although these methods generally yield satisfactory performance, they often introduce additional representation transformation times and involve relatively large model architectures, which can substantially diminish their compatibility with hardware and applications [45]. On the other hand, the sparseness and fine-grained temporal information contained

\*equal contribution. †corresponding author.

1. The Hong Kong University of Science and Technology (Guangzhou)  
2. Guangdong Laboratory of Artificial Intelligence and Digital Economy (SZ)  
3. Carleton University  
4. Shenzhen University

in raw events are greatly discounted when converted into frames and voxels, which is detrimental for tasks like action recognition that rely on critical details in the temporal dimension [41].

Alternative event representation has also been investigated and is gaining popularity. Inspired by PointNet [38] and PointNet++ [39], several studies employ Point Cloud to represent raw events. Such representation exempts the dataformat transformation process, preserves the fine-grained temporal information, and is theoretically coupled with lighter network architectures. However, there are three major limitations preventing Point Cloud-based methods from achieving comparable performance to frame-based and voxel-based methods. Firstly, Point Cloud representation often ignores the polarity information and treats the temporal coordinate  $t$  as a quasi-spatial dimension  $z$  [26, 41, 48], failing to differentiate each dimension of events. Secondly, the Point Cloud networks show a limited performance plateau due to insufficient extraction of spatial-temporal features in the long-term events. Thirdly, the networks’ computational load, which is quantified by the Multiply Accumulate Operations (MACs)[54], super-linear grows with the increase in input points, leading to potential inefficiencies when the input becomes larger [8].

In order to address the constraints mentioned above, we propose an effective and efficient network named FECNet. It leverages Event Cloud representation, which is the nearest representation to raw events and requires only down-sampling. Firstly, we redesign the Group and Sampling (G & S) module to faithfully extract local features incorporating extra polarity information. More specifically, we propose Differentiation Farthest Point Sampling (D-FPS), Event Feature-based K-Nearest Neighbour (EF-KNN), and Coordinates Evolution Strategy (CES). Secondly, we embrace the technique of frequency domain analysis by innovating spatial and temporal Frequency-aware (FA) modules. The Spatial-FA module significantly reduces the MACs by replacing the convolution to Hadamard’s product by a repetition of  $10^4$ . Meanwhile, the Temporal-FA module excels at capturing long-term dependencies of Event Cloud by global frequency filters rather than providing local temporal information. Finally, FECNet can proficiently capture the spatial-temporal features from long-term 2S-1T-1P Event Cloud. We conducted extensive experiments on nine datasets for three different tasks: object classification, action recognition, and human pose estimation. The experimental results sufficiently demonstrate the superiority of FECNet, and the gain in DVS128 Gesture is shown in Fig. 1. Our main contribution can be summarized in the following:

- FECNet pioneer leverages Event Cloud representation, which contains polarity and the nearest to raw output.
- FECNet effectively captures spatial-temporal features

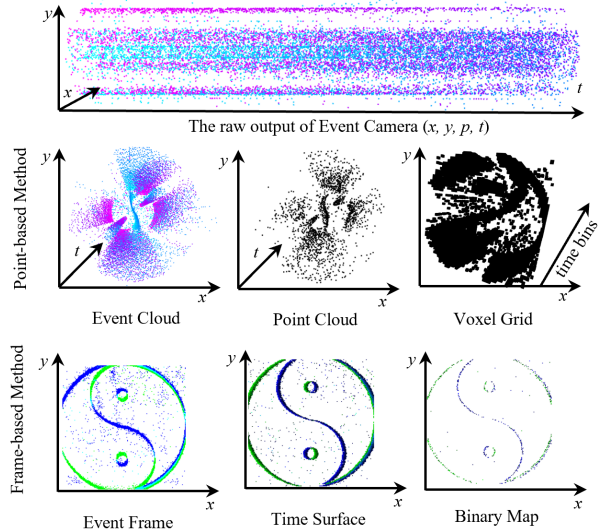


Figure 2. Visualization of different representations in yin-yang from N-Caltech101 dataset.

from long-term events via frequency domain analysis.

- FECNet is capable of handling a greater number of events while being optimized for extremely lightweight.
- Comparable results highlight that FECNet serves as a powerful backbone for the community.

## 2. Related Work

### 2.1. Event Representations

Event cameras capture changes in the environment rather than entire frames at regular intervals, allowing them to record rapid movements with high temporal resolution and perform well in challenging lighting conditions. The representation of output from event cameras is a well-developed research problem [16], and we visualize some frame-based and point-based representations in Fig. 2. The most common one is frame-based representations, which involve converting event streams into 2D frames by either counting the events or summing their polarity over time intervals [6, 17, 20]. However, this representation often results in a loss of temporal information and sparsity since it compresses dynamic information into static images [48]. To address this, Time Surface representations are proposed, which encode the timestamp of the most recent event at each pixel location, thereby maintaining some temporal dynamics [47]. Additionally, Bina-Rep converts asynchronous events to a sequence of sparse and expressive event frames [2], while it is very time-consuming. Another advanced method is voxel-based representation, which segments the event data into multiple time bins, further capturing temporal features across 3D voxel grids that are beneficial for

tasks like 3D reconstruction or depth estimation [4, 14, 51]. Additionally, Point Cloud representation takes a different approach by representing the event data in a 3D spatial format, where each event’s spatial and temporal attributes are preserved [25, 41, 43, 44, 48]. However, this representation ignores polarity and generally has a limited point number. Consequently, we embrace Event Cloud representation closest to the raw output, which only needs downsampling.

## 2.2. Frequency-aware Learning

The Fourier transform is a powerful processing tool in computer vision. With the rapid advancement of convolutional neural networks, the theoretically substitutable frequency-domain Hadamard product offers superior global capture capability and computational efficiency. Initially, FFC employed local Fourier units instead of traditional convolutions, performing convolution operations in the frequency domain to process image features at different scales effectively [11]. Subsequently, GFNet introduced a new technique that enhances feature expression by conducting element-wise multiplication between frequency domain features and learnable global filters [40]. SpectFormer enhanced the feature representation capabilities of the original ViT [15] architecture by combining spectral analysis with multi-head self-attention mechanisms [36]. Recently, network architectures based on frequency domain modules have been extensively applied to various sub-tasks, such as super-resolution [9, 23, 53], low-level tasks [31, 32, 55], and human pose estimation [57]. Event Cloud is a collection of long-term signals containing rich spatial and temporal information, and the utilization of frequency-domain feature extraction can better capture the global temporal relationship between events and conduct lightweight networks.

## 3. Method

### 3.1. Event Cloud Representation

Event cameras generate 2-spatial, 1-temporal, and 1-polarity (2S-1T-1P) raw events in response to illumination changes in the environment. The raw events  $\mathcal{E}$  can be defined as:

$$\mathcal{E} = \{e_i = (x_i, y_i, t_i, p_i) \mid i \in I\}, I = [1, 2, \dots, n], \quad (1)$$

Where  $(x, y)$  represents the spatial coordinate where the event emits,  $t$  denotes the timestamps,  $p$  means the polarity, and  $i$  is the index representing  $i_{\text{th}}$  element in the event stream. As described in Section 2.1,  $\mathcal{E}$  can be transformed into many representations. Still, Event Cloud is the closest representation to raw output and only requires downsampling. Event Cloud can be generated by:

$$\mathcal{EC} = \{e_j = (x_j, y_j, t_j, p_j) \mid j \in J\}, J \subseteq_{\text{ord}} I \quad (2)$$

where  $J$  is a sequential subset of  $I$ , and the length of  $J$  is the number of downsampling points. We define the length of  $J$  as  $T$ , so the dimension of  $\mathcal{EC}$  is  $[T, 4]$ . Specific settings for each dataset are shown in Table 1. It is crucial to emphasize that Event Cloud does not exhibit the permutation invariance characteristic of Point Cloud. So, the sampled events are arranged in the chronological order of their occurrence, enabling the network to extract explicit events’ temporal features subsequently. Finally, Event Cloud is normalized and sent into the network.

### 3.2. Event-based Grouping & Sampling

Considering the inherent difference in the spatial  $(x, y)$ , temporal  $t$ , and polarity  $p$  four coordinates within Event Cloud, we redesign the Grouping & Sampling (G & S) Module to faithfully extract those by treating them differently. Point-based G & S module serves as the fundamental operation that captures local features with the limited receptive field in the Point Cloud space, akin to the convolutional operation in frame-based architecture. Most previous work has ignored the polarity and considered  $t$  as  $z$  of Point Cloud, where temporal information has been treated as an implicit spatial variable for feature extraction. However, the information represented by 2S-1T-1P is not wholly equivalent to that of Point Cloud. To address this discrepancy, we propose the Event-based G & S Module, the details of which will be discussed below.

Before being fed into the Event-based G & S module, Event Cloud passes through the embedding layer, as shown in the Fig. 3. The coordinates information represented by  $\mathcal{EC}$  with dimension  $[T, 4]$  becomes a high-dimensional feature, defined as  $\mathcal{F}$ , with dimension  $[T, D]$ . Consequently, the inputs to the Event-based G & S Module are both  $\mathcal{EC}$  and  $\mathcal{F}$ . Then, we downsample half events to find the centroid using Farthest Point Sampling (FPS) with the coordinates multiplied by a scaling factor  $\alpha$  to focus on different dimensions. We call this process Differentiation FPS (D-FPS), and this process is formulated by:

$$\mathcal{C} = \text{FPS}(\alpha \cdot \mathcal{EC}), \alpha \in \mathbb{R}^4, \mathcal{C} \in \mathbb{R}^{\frac{T}{2} \times 4} \quad (3)$$

where  $\mathcal{C}$  denotes the centroids’ coordinates, which are utilized to group events. Then, the centroid  $\mathcal{C}$  and features  $\mathcal{F}$  are fed into the K-Nearest Neighbor (KNN) block. Different from previous work utilizing coordinates to find the neighbors, we adopt the distance of events’ features and call this process Event Features-based KNN (EF-KNN), which is formulated by the following:

$$\mathcal{G}, \mathcal{F}_{\mathcal{G}} = \text{KNN}(\mathcal{F}_{\mathcal{C}}, \mathcal{F}), \mathcal{G} \in \mathbb{R}^{\frac{T}{2} \times K \times 4}, \mathcal{F}_{\mathcal{G}} \in \mathbb{R}^{\frac{T}{2} \times K \times D} \quad (4)$$

where  $K$  is the number of events in the group,  $\mathcal{F}_{\mathcal{C}}$  represents the centroids’ feature,  $\mathcal{G}$  denotes the grouped events’ coordinate, and  $\mathcal{F}_{\mathcal{G}}$  means the grouped events’ features. The

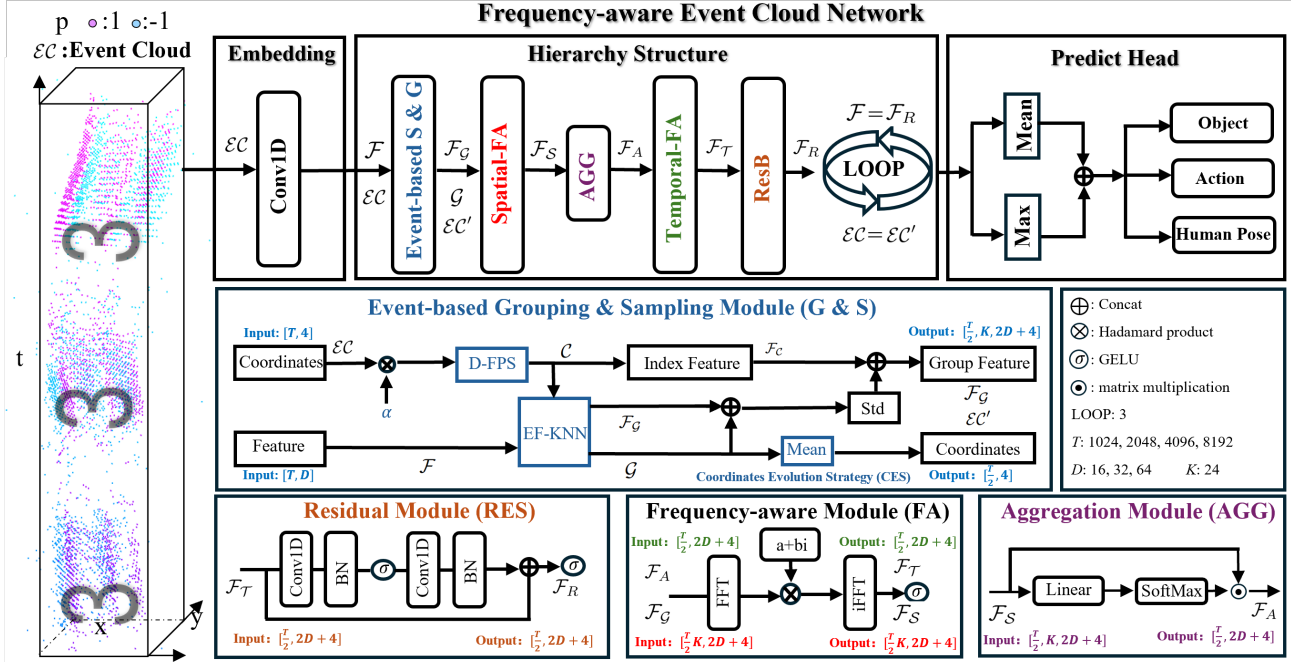


Figure 3. FECNet’s architecture. It accomplishes three tasks by processing the Event Cloud into a sequence of distinct modules: embedding, hierarchy structure, and predict head. In more detail, the hierarchy structure contains five different modules: Event-based G & S module captures the local neighborhood relationships, Spatial-FA abstracts the explicit spatial and implicit temporal features, AGG aggregates the features in a group, Temporal-FA catches the global explicit temporal features, and RES is responsible for the abstraction and high-level representation of features. The final results are obtained by the max-pooling and average-pooling features.

new coordinate is generated by mean operation within the group, and we call this coordinates update process Coordinates Evolution Strategy (CES).

$$\mathcal{EC}' = \text{Mean}(\mathcal{G}), \mathcal{EC}' \in \mathbb{R}^{\frac{T}{2} \times 4} \quad (5)$$

The new group feature is concatenated by two elements:

$$\mathcal{F}_G = \mathcal{F}_G \oplus \mathcal{G}, \mathcal{F}_G \in \mathbb{R}^{\frac{T}{2} \times K \times (D+4)} \quad (6)$$

where  $\oplus$  means the concatenate operation. Finally, the new group feature  $\mathcal{F}_G$  is got under standardized and concatenated with the centroids’ features. The standardized process utilizes the centroids’ feature as mean value:

$$\mathcal{M} = \text{Mean}(\mathcal{F}_G), \mathcal{M} \in \mathbb{R}^{\frac{T}{2} \times (D+4)} \quad (7)$$

$$\mathcal{F}_G = \frac{\mathcal{F}_G - \mathcal{M}}{\text{Std}(\mathcal{F}_G, \mathcal{M})}, \mathcal{F}_G \in \mathbb{R}^{\frac{T}{2} \times K \times (D+4)} \quad (8)$$

$$\mathcal{F}_G = \mathcal{F}_G \oplus \mathcal{F}_C, \mathcal{F}_G \in \mathbb{R}^{\frac{T}{2} \times K \times (2D+4)} \quad (9)$$

where  $\mathcal{M}$  denotes the mean values, and Std is the process to compute the standard deviation.

### 3.3. Frequency-aware Module

We embrace frequency domain analysis to abstract the spatial and temporal features through Spatial Frequency-

aware (FA) modules and Temporal-FA modules, respectively. Event Cloud contains both spatial and temporal information, and the performance is positively correlated to the number of events. Theoretically, more events contain finer temporal information. Nevertheless, capturing the contextual relationships among a large number of events poses a challenge for existing event-based network models, as demonstrated in Tab. 8. Simultaneously, the network has to be lightweight and efficient to match the low power consumption of the event cameras for a wider range of applications. To address the performance plateau and the energy consumption issue with a large number of events, we adopt the Fourier transform for frequency domain feature extraction, with the process formulated as follows.

Different from images, Event Cloud is a one-dimensional signal, as shown in Eq. (2). One-dimensional discrete Fourier Transform (DFT) is employed to convert the Event Cloud features to the frequency domain by the following formulation:

$$X[k] = \sum_{n=0}^{T-1} x[n] e^{-j \frac{2\pi}{T} kn}, \quad k = 0, 1, \dots, T-1 \quad (10)$$

where  $j$  is the imaginary unit,  $x$  represents the signals in the



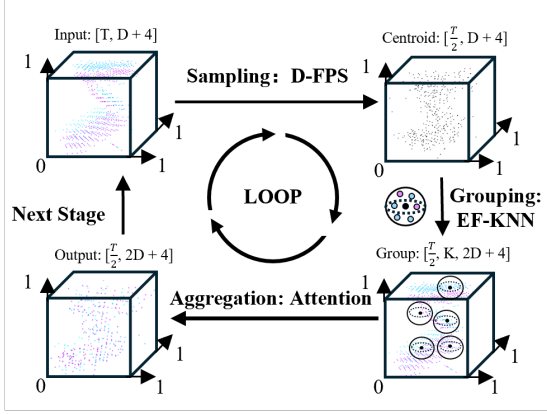


Figure 4. Visualization of Event Cloud’s coordinates and features dimension during hierarchy structure. The closer to the end of the loop, the fewer the number of events and the greater the feature dimension.

temporal domain,  $X$  denotes the spectrum at different frequencies, and  $T$  is the length of temporal signals  $x$ . Additionally, the inverse DFT can recover spectrum to temporal signals by the following formulation:

$$x[n] = \frac{1}{T} \sum_{k=0}^{T-1} X[k] e^{j \frac{2\pi}{T} kn}, \quad n = 0, 1, \dots, T-1 \quad (11)$$

Mathematically, the  $X[T-k] = X^*[k]$ , where  $k \in [0, \frac{T}{2}]$ , it means the spectrum  $X$  is conjugate symmetric. Therefore, the transformed frequency domain spectrum only needs  $\frac{T}{2} + 1$  long enough to be recovered to the original signal.

Once the spectrum is obtained through DFT, we can initialize a learnable filter  $V$  with dimensionality matching that of the spectrum and perform the Hadamard product between the spectrum and the filter. In summary, the specific process of the frequency-aware module is as follows:

$$\begin{aligned} X &= \text{FFT}(x), \\ \hat{X} &= V \odot X, \\ x &= \text{iFFT}(\hat{X}), x = \sigma(x), \end{aligned} \quad (12)$$

where  $\sigma$  is a nonlinear activation function and  $\odot$  means Hadamard product. As shown in Fig. 3, FECNet adopts two different frequency modules, the Spatial-FA module and the Temporal-FA module. They perform Fourier transforms on Event Cloud features in the spatial and temporal dimensions, respectively, and work on extracting spatial and temporal features. The functions of these two modules will be discussed in detail in the following.

**Spatial-FA Module.** In the realm of signal processing, it is theoretically established that convolution in the temporal domain is equivalent to Hadamard’s product in the frequency domain. This equivalence suggests that it is feasible to identify filters in the frequency domain that are

---

### Algorithm 1 FECNet Pipeline

---

**Input:** Event Cloud  $\mathcal{EC}$

**Parameters:** Stage Number:  $m$

**Output:** Category  $\hat{c}$ , Human Pose  $\hat{p}$

- 1:  $\mathcal{F} = \text{Embedding}(\mathcal{EC})$ ,
  - 2: **for**  $i$  in stage( $m$ ) **do**
  - 3:   **Event-based G & S Module**
  - 4:    $\mathcal{G}, \mathcal{F}_G, \mathcal{EC}' = \text{G\&S}(\mathcal{EC}, \mathcal{F})$
  - 5:   **Spatial-FA Module**
  - 6:    $\mathcal{F}_S = \text{SFA}(\mathcal{F}_G)$ ;
  - 7:   **Temporal Aggregate Module**
  - 8:    $\mathcal{F}_A = \text{AGG}(\mathcal{F}_S)$ ;
  - 9:   **Temporal-FA Module**
  - 10:    $\mathcal{F}_T = \text{TFA}(\mathcal{F}_A)$ ;
  - 11:   **ResB Module**
  - 12:    $\mathcal{F}_R = \text{RES}(\mathcal{F}_T)$
  - 13:    $\mathcal{F} = \mathcal{F}_R$ ;  $\mathcal{EC} = \mathcal{EC}'$ ;
  - 14: **end for**
  - 15:  $\mathcal{F} = \text{Mean}(\mathcal{F}) \oplus \text{Max}(\mathcal{F})$
  - 16: **Classifier**            **Regressor**
  - 17: Get category  $\hat{c}$     Get 13 skeleton points  $\hat{p}$
- 

mathematically analogous to those derived through back-propagation with the same performance. The input feature  $\mathcal{F}_G$  to this module is the output of Event-based G & S module, with the dimension  $[\frac{T}{2}, K, 2D + 4]$  as shown in Eq. (9). Previous approaches all employed convolution-based blocks to abstract features across the feature dimensions  $(2D + 4)$ , and this also means doing  $\frac{T}{2} \times K$  repeating calculations. The computational complexity of a single convolution is  $\mathcal{O}((2D + 4)^2)$ . We utilize frequency domain multiplication instead of convolution and the complexity becomes  $\mathcal{O}((2D + 4) \log_2(2D + 4))$ . Taking the dimension 540 of the last stage in FECNet, the individual computational complexity is reduced by a factor of 60. This reduced complexity is finally multiplied by the number of repeats  $\frac{T}{2} \times K \approx 12 \times 10^3$ . The computational complexity reduction by using the spatial-FA module is up to 20 times in the actually constructed network. More importantly, the network’s performance on the various datasets does not give too much of a discount.

**Temporal-FA Module.** FECNet adopts a much larger number of input events ( $T$ ) that is several times as many as in previous Point Cloud-based works. Long-term events have important global and local contextual relationships. Commonly used models like LSTM and attention are not adept at capturing these relationships and would introduce excessive computational complexity as demonstrated in Tab. 8. The input of the Temporal-FA Module is the output of the aggregation module. The aggregation (AGG) module employs a soft attention mechanism on the neighbor dimension to aggregate the feature within a group on

Dataset	Source	Object	Resolution	Train	Test	Point Number	Class	Avg.length (ms)	Sliding Window (ms)
NMNIST [35]	Synthetic	Static	32x32	60000	10000	4096	10	300	300
N-Caltech101 [35]	Synthetic	Static	240x180	20896	5226	8192	101	300	30
CIFAR10-DVS [22]	Synthetic	Static	128x128	99965	24950	10240	10	1280	100
N-Cars [47]	Real	Static	128x128	15422	8607	8192	2	100	100
ASL-DVS [4]	Real	Static	240x180	80640	20160	4096	24	100	100
DVS128 Gesture [1]	Real	Dynamic	128x128	26796	6959	1024	11	6520	500
Daily DVS [28]	Real	Dynamic	346x260	2924	731	8192	12	3000	1500
UCF101-DVS [4]	Synthetic	Dynamic	240x180	108065	27384	8192	101	6600	1000
DHP19 [5]	Real	Dynamic	346x240	124980	24588	4096	13	128	-

Table 1. Specific details of different datasets.

Method	Type	Publish	N-MNIST	N-CARS	CIFAR10-DVS	N-Caltech101	ALS-DVS
Pretrained on ImageNet							
EST [17]	Frame	ICCV'19	0.991	0.925	0.749	0.837	0.991
M-LSTM [6]	Frame	ECCV'20	0.989	0.957	0.73	0.857	0.992
MVF-Net [13]	Frame	TCSVT'21	0.993	0.968	0.762	0.871	0.996
Without Pretraining							
EST [17]	Frame	ICCV'19	0.99	0.919	0.634	0.753	0.979
M-LSTM [6]	Frame	ECCV'20	0.986	0.927	0.631	0.738	0.98
MVF-Net [13]	Frame	TCSVT'21	0.981	0.927	0.599	0.687	0.971
AsyNet [33]	Frame	ECCV'20	-	0.944	0.663	0.745	-
Gabor-SNN [20]	Frame	CVPR'18	0.837	0.789	0.245	0.196	-
HATS [47]	Frame	CVPR'18	0.991	0.902	0.524	0.642	-
ECSNet [10]	Frame	TCSVT'22	0.992	0.946	0.727	0.693	0.997
RG-CNNs [4]	Voxel	TIP'20	0.99	0.914	0.54	0.657	0.901
EV-VGCNN [14]	Voxel	CVPR'22	0.994	<b>0.953</b>	0.651	0.748	0.983
EVTr [52]	Voxel	TCSVT'24	-	0.941	0.731	0.797	0.997
VMV-GCN [51]	Voxel	RAL'22	0.995	0.932	0.69	0.778	0.989
VMST-Net [27]	Voxel	TCSVT'24	0.995	0.944	0.753	0.822	0.998
EventNet [45]	Point Cloud	CVPR'19	0.752	0.75	0.171	0.425	0.833
PointNet++ [39]	Point Cloud	NIPS'17	0.841	0.809	0.465	0.503	0.947
FECNet	Event Cloud	Our	<b>0.997</b>	<b>0.947</b>	<b>0.757</b>	<b>0.824</b>	<b>0.9993</b>

Table 2. Experiment on event-based object classification datasets.

the  $t$  dimension.

$$A = \text{SoftMax}(\text{MLP}(\mathcal{F}_S)), A \in \mathbb{R}^K \quad (13)$$

$$\mathcal{F}_A = \mathcal{F}_S \cdot A, \mathcal{F} \in \mathbb{R}^{\frac{T}{2} \times (2D+4)} \quad (14)$$

where  $A$  is the attention value of group members, and  $\mathcal{F}_S$  is the output of Spatial-FA module. Then, FECNet performs a Fourier transform in the time dimension ( $\frac{T}{2}$ ) of the event features  $\mathcal{F}_A$ . And the temporal features of different frequencies are captured through Eq. (12). The filters  $V$  are global since they can cover all the frequencies and capture both long-term and short-term interactions.

### 3.4. Residual Module

To abstract the higher-level features within the network from Event Cloud, we employ a basic residual module at the end to further enhance the complexity and hierarchy of features. The input and output dimensions of the block are consistent, as shown in Fig. 3.

### 3.5. Overall Architecture

Next, we will present the FECNet pipeline in pseudo-code, utilizing the previously defined variables and formulas as

described in Algorithm 1.

## 4. Experiment

### 4.1. Dataset

We validate FECNet on three tasks nine datasets, e.g., Object Classification: NMNIST [35], N-Caltech101 [35], CIFAR10-DVS [22], N-CARS [47], ASL-DVS [4], Action Recognition: DVS128 Gesture [1], Daily DVS [28], UCF101-DVS [4], Human Pose estimation: DHP19 [5]. For N-Caltech101, CIFAR10-DVS, ASL-DVS, Daily DVS, and UCF101-DVS do not have official divisions, we follow the setting in [4, 10] randomly selected 20% of the samples as the testset, and all other datasets use official divisions. The details of these datasets are shown in Tab. 1.

### 4.2. Implement Details

The hardware platform configuration comprises the following: CPU: AMD 7950x, GPU: RTX 4090. Our training model employs the subsequent set of fixed hyperparameters. Optimizer (AdamW), Initial Learning Rate (0.001), Scheduler (Cosine), and Maximum Epochs (150). The Batch Size

Method	N-Caltech101 [35]	Daily DVS [28]	DHP19 [5]
Event Frame	4.2ms	2.2ms	0.5ms
Binary Map	772ms	286ms	717ms
Time Surface	4.3ms	3.1ms	3.3ms
Voxel Grid	14.6ms	7.9ms	4.3ms
Rasterized Point Cloud	5.8ms	4ms	2.9ms
Event Cloud	<b>1.5ms</b>	<b>1ms</b>	<b>0.3ms</b>

Table 3. Preprocessing time of different representations.

is dynamically set to take full use of the GPU’s memory.

The **Accuracy** metric used in the object classification and action recognition tasks represents the ratio of correctly predicted samples to the total number of samples. The **Mean Per Joint Position Error** (MPJPE) metric is used in the human pose estimation tasks to evaluate the average Euclidean distance between the ground truth and prediction, and the metric space for 2D error is pixels and millimeters for 3D error. The number of skeleton key points set for the experiment is 13.

For all datasets, the hierarchy structure is configured with 3 loops, and the embedding layer is implemented using a single layer of one-dimensional convolution, with input and output dimensions of 4 and 64, respectively. So the dimensional transformation of Event Cloud features is gradually increased to 64, 132, 268, and 540 as the loop goes on, and the formula is calculated as the previous layer’s dimension multiplied by two plus four as demonstrated by Eq. (9). As for the number of groups, which is also the number of centroids in the first loop, NMNIST, N-CARS, DVS128 Gesture, and DHP19 are set to 512, ASL-DVS, Daily DVS, and UCF101-DVS are set to 1024, and CIFAR10-DVS and N-Caltech101 are set to 2048. The number of groups is halved as each loop moves to the next one.

### 4.3. Preprocessing time

We utilize tonic [21] as a code framework, which is a powerful tool for event datasets and transforms. As shown in Tab. 3, the time of preprocessing from raw event output to six representations is required on three datasets. It’s intuitive to see that Event Cloud takes the least amount of time, and this time barely affects the overall throughput of the model. The voxel representations, also equipped with lightweight models, spend a lot of time in data format transformation, nearly 10 times more than Event Cloud.

### 4.4. Object Classification Results

Object classification involves making irregular movements with an event camera around the recognized object, with the classification information primarily encoded in  $(x, y)$  coordinates of the event. Theoretically, stacking events into frames would make it easier to reach the performance plateau. But without the pre-training process of imagenet, the frame-based method performs inferior to the point-

Method	Type	DVSGesture	DailyDVS	UCF101-DVS
TANet [29]	F	0.974	0.963	0.669
I3D [7]	F	0.951	0.909	0.603
ECSNet [10]	F	0.986	-	0.702
TimeSformer [3]	F	0.917	0.906	0.541
RG-CNN [4]	V	0.968	-	0.678
VMV-GCN [51]	V	0.975	0.941	-
VMST-Net [27]	V	0.978	-	0.787
TTPOINT [41]	PC	0.988	0.991	0.725
SpikePoint [42]	PC	0.988	0.979	0.685
FECNet	EC	<b>0.989</b>	<b>0.993</b>	<b>0.916</b>

Table 4. Experiment on event-based action recognition dataset.

based method, which contains the voxel, point cloud, and event cloud as shown in Tab. 2. This is due to the fact that mapping sparse data onto an intensity 2D plane may have aberrations such as ghosting and blurring, which reduces the quality of the dataset. Prior to our work, voxel representations dominated such tasks. Point Cloud does not represent objects well due to the limited number of points it supports (1024 or 2048), resulting in consistently poor performance, which is demonstrated by EventNet and PointNet++. FECNet adopted Event Cloud representation to improve performance by 26% compared to the state-of-the-art (SOTA) Point Cloud method. Even compared with the voxel-based SOTA methods, FECNet shows comparable results on all object classification datasets.

### 4.5. Action Recognition Results

Action recognition is a task used to analyze human movements or gestures. It is widely applied in various fields, including sports, security, and entertainment. This task differs from object classification in that the main information is embedded in the  $t$  coordinates, which represent the type of motion of the observed person or hand. However, voxel-based and frame-based representations tend to diminish the resolution of  $t$ , reducing it from a fine-grained range (1000000) to a coarse-grained range (0 - 40). So, the finer-grained temporal resolution of the representations, the better the performance results, as shown in Tab. 4. FECNet utilizes the finest-grained representation of Event Cloud to fully extract its spatial-temporal features, achieving SOTA results on all three action recognition datasets. Especially on the UCF101-DVS dataset, FECNet far outperforms the previous SOTA methods by 16% named VMST-Net. This implies that critical information you omit in the representations, and you cannot recover or make it up through the network architecture.

In addition, we tested the hardware resource consumption and runtime of FECNet on the server platform. Tab. 5 shows the amazing results of FECNet. Thanks to the design of the Spatial-FA module, FECNet achieves leading results with a remarkably low computational cost, requiring only one-thousandth of the MACs compared to frame-based

Method	Type	Param(M)	MACs(G)	FPS	Accuracy
I3D [7]	F	49.19	59.28	34	0.951
TANet [29]	F	24.80	65.94	32	0.974
TimeSformer [3]	F	121.27	379.70	23	0.967
VMV-GCN [51]	V	0.84	0.33	99	0.975
EVSTr [52]	V	2.88	1.38	41	0.986
RG-CNN [4]	V	19.46	0.4	-	0.968
PointNet [38]	PC	3.46	0.23	455	0.902
PointNet++ [39]	PC	1.48	0.44	415	0.963
TTPOINT [41]	PC	0.334	0.29	88	0.988
FECNet	EC	<b>0.898</b>	<b>0.109</b>	229.7	0.989

Table 5. Hardware benchmark on DVS128 Gesture dataset.

Method	Type	MPJPE <sub>2D</sub>	MPJPE <sub>3D</sub>	Param.	GMACs
Pose-Res50 [50]	F	5.28	59.83	34	12.91
LeVit-128S [18]	F	7.68	87.79	7.87	0.2
DHP19 [5]	F	7.67	87.9	0.22	3.51
VMV-PointTrans [51, 56]	V	9.13	103.23	3.67	5.98
VMST-Net [27]	V	6.45	73.07	3.59	0.38
PointNet [8, 38]	RPC	7.29	82.46	4.46	1.19
DGCNN [8, 49]	RPC	6.83	77.32	4.51	4.91
Point Transformer [8, 56]	RPC	6.46	73.07	3.65	5.03
FECNet	EC	<b>6.11</b>	<b>69.89</b>	<b>1.831</b>	<b>0.161</b>

Table 6. Experiment on event-based human pose estimation dataset. RPC means the rasterized Point Cloud representation [56].

methods. Additionally, FECNet inherits the high inference speed of Point Cloud representations, delivering an impressive throughput of 230 FPS while far superior to frame-based and voxel-based methods. Although the number of parameters in FECNet is higher than that of TTPOINT, the tensor decomposition technique employed significantly reduces the network’s inference time. FECNet still maintains a relatively low parameter count compared to the frame-based method.

## 4.6. Human Pose Estimation Results

Human pose estimation is a fundamental task that is widely used in autonomous driving, virtual reality, and security. It aims to accurately regress the human skeletons’ key points. Event cameras are distinguished by their advantages in privacy, high speed, and ability to capture motion without blur in such tasks. We follow the DHP19 official split setting, using S1-S12 for training and S13-S17 for testing, and only two front cameras are used following the raw DHP19 dataset. Point Cloud representation was demonstrated to be efficient for edge devices but did not perform well in the MPJPE metric [56]. Furthermore, this work proposed the Rasterized Point Cloud representation (RPC), which retains the original Point Cloud network while additionally introducing the representation transformation time, as shown in Tab. 3. FECNet leverages the raw unprocessed Event Cloud to reach the SOTA results of point-based and voxel-based methods. Meanwhile, FECNet has the smallest model size, with GMACs of only 0.12, which is 2% of Point Transformer. In addition, it takes only 4.37 ms for the model to

Dataset	DHP19 [5]		N-CARS [47]	UCF101-DVS [4]
Metric	MPJPE <sub>2D</sub>	MPJPE <sub>3D</sub>	Acc.	Acc.
w all	<b>6.11</b>	<b>69.89</b>	<b>0.947</b>	<b>0.916</b>
w point-based G & S	6.27	71.12	0.937	0.913
w/o TFT	6.47	73.84	0.944	0.913
w/o polarity	6.19	70.30	0.944	0.911

Table 7. Ablation study on three different tasks with core modules.

Event number	FECNet	FECNet w LSTM	PointNet++ [39]	TTPOINT [41]
512	46.29	44.16	37.63	39.70
1024	50.36	48.31	43.54	42.15
2048	52.24	49.10	47.02	42.58
4096	56.57	50.84	49.04	44.39
8192	60.04	53.63	53.15	43.65
10240	60.60	52.42	54.39	45.61

Table 8. Ablation study of different Point-based networks in N-Caltech101 with 300 ms sliding window.

infer a sample on the server.

## 4.7. Ablation Study

### 4.7.1. Modules Ablation

“w point-based G & S” means FECNet adopts the vanilla Grouping and Sampling module design for the Point Cloud area, which treats  $(x, y, p, t)$  all the same. The performance of the model decreased on all three datasets. “w/o TFT” denotes that FECNet is not equipped with the Temporal-FA module for extracting explicit feature extraction. The model showed a significant decrease on the DHP19 dataset, suggesting that temporal features are important for predicting the human skeleton. “w/o polarity” represents the input equal to the Point Cloud representation. All three datasets have demonstrated that polarity provides additional information and brings performance improvements.

### 4.7.2. Event Number

PointNet++ and TTPOINT do not have an explicit temporal feature extraction module, the accuracy is much lower than that of FECNet, and the performance of TTPOINT does not improve clearly after 4096 points as shown in Tab. 8. Additionally, FECNet utilizes LSTM for temporal feature extraction, which makes it difficult to capture long-term dependencies between events as the number of points grows.

## 5. Conclusion

In this paper, we utilize Event Cloud representation, which is the nearest one to the raw events. In order to effectively and efficiently extract long-term events’ features, we propose event-based G & S modules and embrace frequency domain analysis. We benchmark FECNet on nine datasets from three tasks, and the ground-breaking results show promise with Frequency-aware Event Cloud Network.



## References

- [1] Arnon Amir, Brian Taba, David Berg, Timothy Melano, Jeffrey McKinstry, Carmelo Di Nolfo, Tapan Nayak, Alexander Andreopoulos, Guillaume Garreau, Marcela Mendoza, et al. A low power, fully event-based gesture recognition system. In *Proceedings of the IEEE conference on computer vision and pattern recognition*, pages 7243–7252, 2017. 6
- [2] Sami Barchid, José Mennesson, and Chaabane Djéraba. Bina-rep event frames: A simple and effective representation for event-based cameras. In *2022 IEEE International Conference on Image Processing (ICIP)*, pages 3998–4002. IEEE, 2022. 2
- [3] Gedas Bertasius, Heng Wang, and Lorenzo Torresani. Is space-time attention all you need for video understanding? In *ICML*, page 4, 2021. 7, 8
- [4] Yin Bi, Aaron Chadha, Alhabib Abbas, Eirina Bourtsoulatze, and Yiannis Andreopoulos. Graph-based spatio-temporal feature learning for neuromorphic vision sensing. *IEEE Transactions on Image Processing*, 29:9084–9098, 2020. 3, 6, 7, 8
- [5] Enrico Calabrese, Gemma Taverni, Christopher Awai Easthope, Sophie Skriabine, Federico Corradi, Luca Longinotti, Kynan Eng, and Tobi Delbruck. Dhp19: Dynamic vision sensor 3d human pose dataset. In *Proceedings of the IEEE/CVF conference on computer vision and pattern recognition workshops*, pages 0–0, 2019. 6, 7, 8
- [6] Marco Cannici, Marco Ciccone, Andrea Romanoni, and Matteo Matteucci. A differentiable recurrent surface for asynchronous event-based data. In *Computer Vision—ECCV 2020: 16th European Conference, Glasgow, UK, August 23–28, 2020, Proceedings, Part XX 16*, pages 136–152. Springer, 2020. 2, 6
- [7] Joao Carreira and Andrew Zisserman. Quo vadis, action recognition? a new model and the kinetics dataset. In *proceedings of the IEEE Conference on Computer Vision and Pattern Recognition*, pages 6299–6308, 2017. 7, 8
- [8] Jiaan Chen, Hao Shi, Yaozu Ye, Kailun Yang, Lei Sun, and Kaiwei Wang. Efficient human pose estimation via 3d event point cloud. In *2022 International Conference on 3D Vision (3DV)*, pages 1–10. IEEE, 2022. 2, 8
- [9] Jiadi Chen, Chunjiang Duanmu, and Huanhuan Long. Large kernel frequency-enhanced network for efficient single image super-resolution. In *Proceedings of the IEEE/CVF Conference on Computer Vision and Pattern Recognition*, pages 6317–6326, 2024. 3
- [10] Zhiwen Chen, Jinjian Wu, Junhui Hou, Leida Li, Weisheng Dong, and Guangming Shi. Ecsnet: Spatio-temporal feature learning for event camera. *IEEE Transactions on Circuits and Systems for Video Technology*, 33(2):701–712, 2022. 6, 7
- [11] Lu Chi, Borui Jiang, and Yadong Mu. Fast fourier convolution. *Advances in Neural Information Processing Systems*, 33:4479–4488, 2020. 3
- [12] Tobi Delbruck and Manuel Lang. Robotic goalie with 3 ms reaction time at 4% cpu load using event-based dynamic vision sensor. *Frontiers in neuroscience*, 7:223, 2013. 1
- [13] Yongjian Deng, Hao Chen, and Youfu Li. Mvf-net: A multi-view fusion network for event-based object classification. *IEEE Transactions on Circuits and Systems for Video Technology*, 32(12):8275–8284, 2021. 6
- [14] Yongjian Deng, Hao Chen, Hai Liu, and Youfu Li. A voxel graph cnn for object classification with event cameras. In *Proceedings of the IEEE/CVF Conference on Computer Vision and Pattern Recognition*, pages 1172–1181, 2022. 3, 6
- [15] Alexey Dosovitskiy. An image is worth 16x16 words: Transformers for image recognition at scale. *arXiv preprint arXiv:2010.11929*, 2020. 1, 3
- [16] Guillermo Gallego, Tobi Delbrück, Garrick Orchard, Chiara Bartolozzi, Brian Taba, Andrea Censi, Stefan Leutenegger, Andrew J Davison, Jörg Conradt, Kostas Daniilidis, et al. Event-based vision: A survey. *IEEE transactions on pattern analysis and machine intelligence*, 44(1):154–180, 2020. 1, 2
- [17] Daniel Gehrig, Antonio Loquercio, Konstantinos G Derpanis, and Davide Scaramuzza. End-to-end learning of representations for asynchronous event-based data. In *Proceedings of the IEEE/CVF International Conference on Computer Vision*, pages 5633–5643, 2019. 2, 6
- [18] Benjamin Graham, Alaaeldin El-Nouby, Hugo Touvron, Pierre Stock, Armand Joulin, Hervé Jégou, and Matthijs Douze. Levit: a vision transformer in convnet’s clothing for faster inference. In *Proceedings of the IEEE/CVF international conference on computer vision*, pages 12259–12269, 2021. 8
- [19] Kaiming He, Xiangyu Zhang, Shaoqing Ren, and Jian Sun. Deep residual learning for image recognition. In *Proceedings of the IEEE conference on computer vision and pattern recognition*, pages 770–778, 2016. 1
- [20] Jun Haeng Lee, Tobi Delbruck, and Michael Pfeiffer. Training deep spiking neural networks using backpropagation. *Frontiers in neuroscience*, 10:508, 2016. 2, 6
- [21] Gregor Lenz, Kenneth Chaney, Sumit Bam Shrestha, Omar Oubari, Serge Picaud, and Guido Zarrella. Tonic: Event-based datasets and transformations., 2021. Documentation available under <https://tonic.readthedocs.io>. 7
- [22] Hongmin Li, Hanchao Liu, Xiangyang Ji, Guoqi Li, and Luping Shi. Cifar10-dvs: an event-stream dataset for object classification. *Frontiers in neuroscience*, 11:309, 2017. 6
- [23] Junxuan Li, Shaodi You, and Antonio Robles-Kelly. A frequency domain neural network for fast image super-resolution. In *2018 International Joint Conference on Neural Networks (IJCNN)*, pages 1–8. IEEE, 2018. 3
- [24] Patrick Lichtsteiner, Christoph Posch, and Tobi Delbruck. A  $128 \times 128$  120 db 15  $\mu$ s latency asynchronous temporal contrast vision sensor. *IEEE journal of solid-state circuits*, 43(2):566–576, 2008. 1
- [25] Xiaopeng Lin, Hongwei Ren, and Bojun Cheng. Fapnet: An effective frequency adaptive point-based eye tracker. In *Proceedings of the IEEE/CVF Conference on Computer Vision and Pattern Recognition*, pages 5789–5798, 2024. 3

- [26] Xiaopeng Lin, Hongwei Ren, Yulong Huang, Zunchang Liu, Yue Zhou, Haotian Fu, Biao Pan, and Bojun Cheng. Event-based motion deblurring via multi-temporal granularity fusion. *arXiv preprint arXiv:2412.11866*, 2024. 2
- [27] Daikun Liu, Teng Wang, and Changyin Sun. Voxel-based multi-scale transformer network for event stream processing. *IEEE Transactions on Circuits and Systems for Video Technology*, 2023. 6, 7, 8
- [28] Qianhui Liu, Dong Xing, Huajin Tang, De Ma, and Gang Pan. Event-based action recognition using motion information and spiking neural networks. In *IJCAI*, pages 1743–1749, 2021. 6, 7
- [29] Zhaoyang Liu, Limin Wang, Wayne Wu, Chen Qian, and Tong Lu. Tam: Temporal adaptive module for video recognition. In *Proceedings of the IEEE/CVF international conference on computer vision*, pages 13708–13718, 2021. 7, 8
- [30] Fei Ma, Yukan Li, Yifan Xie, Ying He, Yi Zhang, Hongwei Ren, Zhou Liu, Wei Yao, Fuji Ren, Fei Richard Yu, et al. A review of human emotion synthesis based on generative technology. *arXiv preprint arXiv:2412.07116*, 2024. 1
- [31] Xintian Mao, Yiming Liu, Fengze Liu, Qingli Li, Wei Shen, and Yan Wang. Intriguing findings of frequency selection for image deblurring. In *Proceedings of the AAAI Conference on Artificial Intelligence*, pages 1905–1913, 2023. 3
- [32] Xintian Mao, Jiansheng Wang, Xingran Xie, Qingli Li, and Yan Wang. Loforner: Local frequency transformer for image deblurring. In *ACM Multimedia 2024*, 2024. 3
- [33] Nico Messikommer, Daniel Gehrig, Antonio Loquercio, and Davide Scaramuzza. Event-based asynchronous sparse convolutional networks. In *Computer Vision—ECCV 2020: 16th European Conference, Glasgow, UK, August 23–28, 2020, Proceedings, Part VIII 16*, pages 415–431. Springer, 2020. 6
- [34] Elias Mueggler, Henri Rebecq, Guillermo Gallego, Tobi Delbruck, and Davide Scaramuzza. The event-camera dataset and simulator: Event-based data for pose estimation, visual odometry, and slam. *The International Journal of Robotics Research*, 36(2):142–149, 2017. 1
- [35] Garrick Orchard, Ajinkya Jayawant, Gregory K Cohen, and Nitish Thakor. Converting static image datasets to spiking neuromorphic datasets using saccades. *Frontiers in neuroscience*, 9:437, 2015. 6, 7
- [36] Badri N Patro, Vinay P Namboodiri, and Vijay Srinivas Agneeswaran. Spectformer: Frequency and attention is what you need in a vision transformer. *arXiv preprint arXiv:2304.06446*, 2023. 3
- [37] Christoph Posch, Daniel Matolin, and Rainer Wohlgenannt. A qvga 143 db dynamic range frame-free pwm image sensor with lossless pixel-level video compression and time-domain cds. *IEEE Journal of Solid-State Circuits*, 46(1):259–275, 2010. 1
- [38] Charles R Qi, Hao Su, Kaichun Mo, and Leonidas J Guibas. Pointnet: Deep learning on point sets for 3d classification and segmentation. In *Proceedings of the IEEE conference on computer vision and pattern recognition*, pages 652–660, 2017. 2, 8
- [39] Charles Ruizhongtai Qi, Li Yi, Hao Su, and Leonidas J Guibas. Pointnet++: Deep hierarchical feature learning on point sets in a metric space. *Advances in neural information processing systems*, 30, 2017. 2, 6, 8
- [40] Yongming Rao, Wenliang Zhao, Zheng Zhu, Jiwen Lu, and Jie Zhou. Global filter networks for image classification. *Advances in neural information processing systems*, 34:980–993, 2021. 3
- [41] Hongwei Ren, Yue Zhou, Haotian Fu, Yulong Huang, Renjing Xu, and Bojun Cheng. Ttpoint: A tensorized point cloud network for lightweight action recognition with event cameras. In *Proceedings of the 31st ACM International Conference on Multimedia*, pages 8026–8034, 2023. 2, 3, 7, 8
- [42] Hongwei Ren, Yue Zhou, LIN Xiaopeng, Yulong Huang, FU Haotian, Jie Song, and Bojun Cheng. Spikepoint: An efficient point-based spiking neural network for event cameras action recognition. In *The Twelfth International Conference on Learning Representations*, 2024. 7
- [43] Hongwei Ren, Yue Zhou, Jiadong Zhu, Haotian Fu, Yulong Huang, Xiaopeng Lin, Yuetong Fang, Fei Ma, Hao Yu, and Bojun Cheng. Rethinking efficient and effective point-based networks for event camera classification and regression: Eventmamba. *arXiv preprint arXiv:2405.06116*, 2024. 3
- [44] Hongwei Ren, Jiadong Zhu, Yue Zhou, Haotian Fu, Yulong Huang, and Bojun Cheng. A simple and effective point-based network for event camera 6-dofs pose relocation. In *Proceedings of the IEEE/CVF Conference on Computer Vision and Pattern Recognition*, pages 18112–18121, 2024. 3
- [45] Yusuke Sekikawa, Kosuke Hara, and Hideo Saito. Eventnet: Asynchronous recursive event processing. In *Proceedings of the IEEE/CVF conference on computer vision and pattern recognition*, pages 3887–3896, 2019. 1, 6
- [46] Karen Simonyan and Andrew Zisserman. Very deep convolutional networks for large-scale image recognition. *arXiv preprint arXiv:1409.1556*, 2014. 1
- [47] Amos Sironi, Manuele Brambilla, Nicolas Bourdis, Xavier Lagorce, and Ryad Benosman. Hats: Histograms of averaged time surfaces for robust event-based object classification. In *Proceedings of the IEEE conference on computer vision and pattern recognition*, pages 1731–1740, 2018. 2, 6, 8
- [48] Qinyi Wang, Yexin Zhang, Junsong Yuan, and Yilong Lu. Space-time event clouds for gesture recognition: From rgb cameras to event cameras. In *2019 IEEE Winter Conference on Applications of Computer Vision (WACV)*, pages 1826–1835. IEEE, 2019. 1, 2, 3
- [49] Yue Wang and Justin M Solomon. Object dgcnn: 3d object detection using dynamic graphs. *Advances in Neural Information Processing Systems*, 34:20745–20758, 2021. 8
- [50] Bin Xiao, Haiping Wu, and Yichen Wei. Simple baselines for human pose estimation and tracking. In *Proceedings of the European conference on computer vision (ECCV)*, pages 466–481, 2018. 8
- [51] Bochen Xie, Yongjian Deng, Zhanpeng Shao, Hai Liu, and Youfu Li. Vmv-gcn: Volumetric multi-view based graph cnn for event stream classification. *IEEE Robotics and Automation Letters*, 7(2):1976–1983, 2022. 3, 6, 7, 8

- [52] Bochen Xie, Yongjian Deng, Zhanpeng Shao, Qingsong Xu, and Youfu Li. Event voxel set transformer for spatiotemporal representation learning on event streams. *IEEE Transactions on Circuits and Systems for Video Technology*, 2024. 6, 8
- [53] Shengke Xue, Wenyuan Qiu, Fan Liu, and Xinyu Jin. Faster image super-resolution by improved frequency-domain neural networks. *Signal, Image and Video Processing*, 14(2): 257–265, 2020. 3
- [54] Ziyi Yang, Kehan Liu, Yiru Duan, Mingjia Fan, Qiyue Zhang, and Zhou Jin. Three challenges in ream-based process-in-memory for neural network. In *2023 IEEE 5th International Conference on Artificial Intelligence Circuits and Systems (AICAS)*, pages 1–5. IEEE, 2023. 2
- [55] Hu Yu, Naishan Zheng, Man Zhou, Jie Huang, Zeyu Xiao, and Feng Zhao. Frequency and spatial dual guidance for image dehazing. In *European Conference on Computer Vision*, pages 181–198. Springer, 2022. 3
- [56] Hengshuang Zhao, Li Jiang, Jiaya Jia, Philip HS Torr, and Vladlen Koltun. Point transformer. In *Proceedings of the IEEE/CVF international conference on computer vision*, pages 16259–16268, 2021. 8
- [57] Qitao Zhao, Ce Zheng, Mengyuan Liu, Pichao Wang, and Chen Chen. Poseformerv2: Exploring frequency domain for efficient and robust 3d human pose estimation. In *Proceedings of the IEEE/CVF Conference on Computer Vision and Pattern Recognition*, pages 8877–8886, 2023. 3